A Data-Driven Approach for Estimating Inertia and Damping of a Single-Area Power System

Bimal Pandey, Dilip Pandit, Nga Nguyen
Electrical Engineering & Computer Science, University of Wyoming, Laramie, WY, 82071
{bpandey1, dpandit, nga.nguyen}@uwyo.edu

***Abstract*—The inertia of the electrical grid is crucial for ensuring system stability. The increasing integration of renewable energy resources gradually decreases the inertia of the system, leading to greater frequency deviation under disturbances. Similarly, due to fluctuating demand and intermittent generation, system inertia varies considerably. In this context, the accurate estimation of inertia is crucial which is challenging through conventional mathematical methods. This paper proposes a convolution neural network approach for estimating the inertia and damping of an electrical grid. The neural network-based method utilizes a non-disruptive test signal to change the dynamics of the power network and estimates the system inertia and damping coefficient from the local frequency measurements. The introduced method determines the inertia and damping with high accuracy even under the impact of noise and is compared with the performance of the multilayer perceptron, support vector machine regressor, and gradient-boosting machine regressor in terms of accuracy, root mean squared error, and mean absolute error to validate the results. The proposed technique can assist system operators in providing fast-frequency support and system protection schemes.**

***Index Terms*—Convolution neural network, fluctuating demand, frequency support, renewable energy resources.**

I. Introduction

The imbalance between electric power supply and consumption, including system losses, causes deviations in the system's frequency. Frequency deviation needs to be maintained within a certain range for the reliable functioning of the grid. The inability to return the system to equilibrium after the disturbances might increase the chance of under-frequency load-shedding and cascading failures [1], [2]. Inertia has a direct impact on frequency deviation when the system encounters disturbances. Therefore, it can function as an indicator to determine the severity level of disturbances that a system can tolerate.

With the growing penetration of converter-dominated generation, conventional synchronous generators are gradually decommissioned. This leads to a reduction in system inertia as the overall inertial contribution of converter-based generation is negligible to date [3]. In addition, the use of asynchronous high voltage direct current (HVDC) divides the large power grids into multiple sub-grids, weakening grid inertia and decreasing frequency support among AC grids [4]. Under these circumstances, conventional frequency control techniques are inadequate to address the changing disturbance dynamics [5]. As a result, a series of failures and disconnections can occur requiring faster primary control to preserve stability.

Moreover, the gradual increment of deregulated and unpredictable energy generation is making inertia a dynamic parameter changing continuously over time and introducing non-linearity in the system operation [6]. Therefore, it is difficult for the transmission system operator (TSO) to accurately monitor the system inertia [7], [8]. This limitation requires excessively cautious operational planning and drives up operational expenses. Hence, accurate inertia estimation techniques help TSOs operate the system with lower safety margins and costs by implementing the appropriate actions and control strategies. Moreover, inertia and damping constant estimation have significant advantages including regulated incorporation of renewable energy resources (RERs), increased stability and reliability, and improved market structuring for ancillary services.

In [9], the waveform of the transients has been used for determining the inertia through a polynomial approximation to time. However, the order of polynomials was selected based on the specific dataset. In [10], an improved approach is established by improving the polynomial approximation that estimates the inertia constant using frequency information captured by phasor measurement units (PMUs). However, PMU data is limited to specific areas like points of common coupling making this approach unfit for different areas. In [11], the statistical method is formulated using the Gaussian Markov model which estimates the inertia in near real-time inertia by analyzing steady-state conditions and minor frequency variations. This method requires the collection of past system data for accurate predictions which makes it less efficient for an intermediate sampling interval. The Bayesian inference technique is proposed in [12] which depends upon the posterior probability density function of the events. This approach is statistically difficult and less suitable for large systems. In [13], inertia is estimated using an extended Kalman filter but this approach needs to assume the time of disturbances and is sensitive to the used time of the filter.

An analytical method using a dynamic mode decomposition is used to estimate inertia for interconnected power grids in [14]. However, the dependency on eigenvalues and eigenvectors for estimation makes it less reliable in multi-area systems. In [15], the closed-loop estimation procedure is implemented for predicting the inertia at the connection bus. The measurement unit measures the required frequency and active power for the feedback-based estimation technique. However, this method has a higher level of complexity and is highly sensitive to noise. The authors in [16] have introduced a time-dependent inertia estimation technique that requires an actual time of perturbation in the system. This method

might be infeasible to implement due to the uncertainty of load fluctuation in the real world. In [17], inertia estimation dependent on electromechanical oscillation was implemented using iterative filtering. However, his method relies heavily on statistical calculation and suffers from higher noise. This issue is partly resolved by [18], where a noise-resistant data-driven approach for inertia estimation is developed.

Most of the previous methods rely on mathematical model-based inertia estimation. Very few studies have focused on a model-free data-centric approach that can capture the uncertainty of modern grids. Similarly, the damping constant estimation has been ignored in the previous works which need to be considered for the real-time assessment and deployment of control strategies for effective response to disturbances. Therefore, this paper presents a data-driven approach that does not depend on predefined models for predicting system inertia and damping constant using a convolution neural network. The contributions of this paper are described below.

1) Develop a micro perturbation-based technique for estimating system inertia and damping constant using a convolution neural network. The proposed approach utilizes frequency measurements obtained from arbitrary disturbances that occur in the system for estimating these parameters of the system. Hyperparameter optimization is done to ensure the optimal performance of the CNN model.
2) The proposed technique will consider the influence of measurement noise on inertia and damping constant estimation. This has been ignored in most existing works.

The remaining work of the paper is as follows. An overview of the frequency dynamics of single-area power networks is explained in Section II. Section III describes the concepts of a convolution neural network and its utilization for estimating inertia and damping constant. A simulation model and results are described in section IV. The conclusion is in Section V.

II. Power System Frequency Dynamics

The inertia and damping constant are estimated considering a single-area power grid. The transfer function-based model is used to represent the system dynamics. Synchronous generators are considered the main source of power generation. All the generating units of the single-area network are represented by one equivalent generator. This simplifies the overall problem and the frequency response can be represented by the swing equation [19], [20].

A. Swing Equation: Inertia and Damping Constant

Multiple generators that are interconnected in the single area network will serve the load according to the consumption level. The frequency and inertia can be represented in terms of center of inertia (COI) [21]. Thus, the average frequency is defined as follows:

$$\omega = \sum_{k=1}^{N_g} \frac{H_k \omega_k}{H} \tag{1}$$

where H_k and w_k are the inertia constant and angular frequency of k^{th} generator. The number of generators is denoted by N_g. The inertia constant H is defined as:

$$H = \sum_{k=1}^{N_g} \frac{H_k S_k}{S} \tag{2}$$

S_k denotes apparent power rating. From these above equations, the swing equation of the single area can be modeled as follows [22]:

$$\Delta\dot{\omega} = \frac{\omega_0}{2H} \frac{(\Delta P_m - \Delta P_l)}{S} \tag{3}$$

$$M\Delta\dot{\omega} + D\Delta\omega = \Delta P_m - \Delta P_l \tag{4}$$

$\Delta\omega$ indicates average frequency deviation. $\Delta\dot{\omega}$ gives the rate of change of frequency (ROCOF), and $M = 2H$ is the inertia constant of the equivalent generator. ΔP_m and ΔP_l denote a change in mechanical and electrical power output, respectively, damping constant, D represents the impacts of frequency-dependent loads and other damping mechanisms. Typically, D indicates the percentage change in load resulting from a 1% change in the system's frequency.

B. Frequency Control Loop

The turbine-governor and load-generator dynamics for the frequency control of the single-area electrical grid are illustrated in Fig. 1. An abrupt change of load triggers the frequency event which is initially responded to through the primary control. The turbine-governor dynamics act to bring the system to a stable condition.

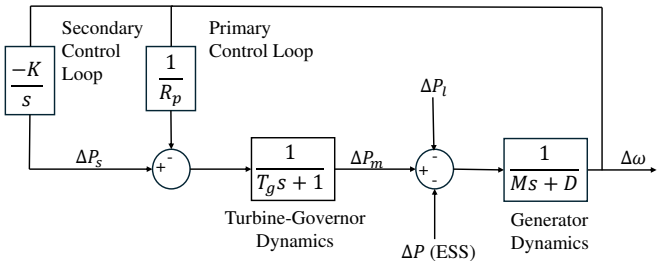

Fig. 1: Frequency control loop of single area power system.

The secondary frequency control loop reinstates the system frequency to its original form after disturbances. The integral controller block integrates the accumulated frequency deviation over time to ensure the secondary control removes the steady-state error, thus restoring the nominal frequency. In Fig. 1, K_i represents the proportional gain, T_g denotes the turbine-generator time constant, and the block $\frac{1}{R_p}$ is speed-regulation droop. This system is subjected to disturbances to obtain the frequency measurements for the implementation of CNN.

A probing signal can be applied to the power system without affecting the system stability to understand system dynamics. In this work, an excitation signal ΔP_l is employed for perturbing the above-modeled power system to study the frequency dynamics and system inertia. The following

test signal consists of pulses with amplitude and frequency equivalent to 0.01 p.u. and 1Hz, respectively. Fig. 2. shows the resulting measurements of $\Delta\omega$ and $\Delta\dot{\omega}$ for these values. Multiple samples for $\Delta\omega$ and $\Delta\dot{\omega}$ are obtained using the different values of M, ΔP_l, and D. The Gaussian noise is introduced to mimic the measurements noise in $\Delta\omega$ and $\Delta\dot{\omega}$. Once multiple samples of $\Delta\omega$ and $\Delta\dot{\omega}$ are obtained, the sampling time is defined to estimate the inertia in which the inertial response is significant.

III. Convolution Neural Network for Inertia and Damping Estimation

A convolution neural network is a multi-layered neural network capable of dealing with sequential data models. Other neural network architectures such as long short-term memory (LSTM) can also deal with sequential data models. However, CNNs can excel the LSTM at capturing local patterns in data using convolution filters. The accelerated learning capabilities of CNNs have been one of the key features for its extensive use over LSTM [23]. This work uses 1D-CNN to predict the inertia and damping in a single-area power network. The convolution layers in the CNN have the good property of extracting sequential features that make CNN suitable for inertia and damping estimation.

The architecture of the 1D-CNN network implemented in this paper is illustrated in Fig. 3. The frequency variations data, $\Delta\omega$ and $\Delta\dot{\omega}$ derived from the simulation setting of Fig. 1 are used as the input features to train the CNN. In the first stage, the datasets are categorized into training and testing data during the training process, and the input features are selected randomly from the entire dataset with batch size b. The input features, $\Delta\omega$ and $\Delta\dot{\omega}$ are placed horizontally making the input $b \times c$ to the first convolution layer. The process of batch training is completed only when all the batches of $\Delta\omega$ and $\Delta\dot{\omega}$ are fully trained to predict the inertia and damping constant. During the forward propagation, these input features are passed to convolution layers where sequential features of datasets are extracted. The convolution layer responds with feature mapping, where each output comprises several convolution results of inputted feature figures. In this section, the sequential features of $\Delta\omega$ and $\Delta\dot{\omega}$ are learned by the convolution filters or kernels of the convolution layer. Each convolution layer is composed of kernel vectors that map the input features. Similarly, each convolution layer consists of another parameter called channels which are denoted by p and q as shown in Fig. 3. The kernel size and number of channels together serve as the hyperparameter for the convolution layer, whose values are optimized for best performance of the model.

The dense layer receives the processed features from convolution layer kernels. The convolution layer consists of a series of convolution filters, also called kernels, that act across the input features to capture the temporal dependencies at different intervals of time and learn the relevant features. Similarly, these layers transform the 2D feature data into 1D, ensuring all neurons are fully connected to the final layer. This flattened layer Y as shown in Fig. 3 is connected to the output layer via

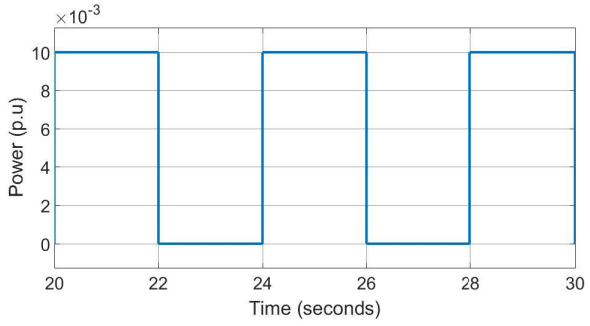

(a)

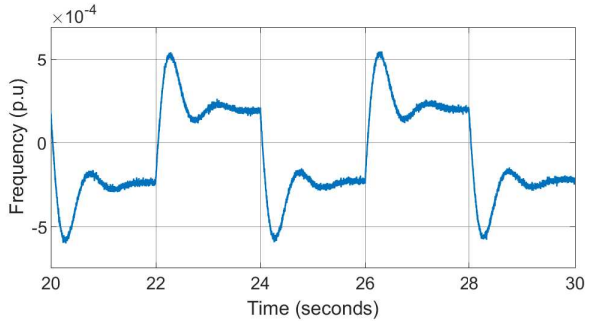

(b)

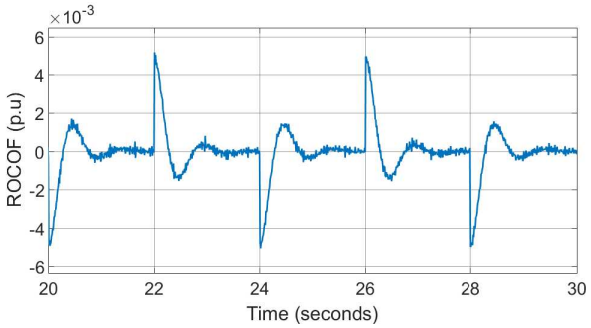

(c)

Fig. 2: Probing signal, frequency, and ROCOF measurements for M= 2s and $\Delta P_l = 0.01$.

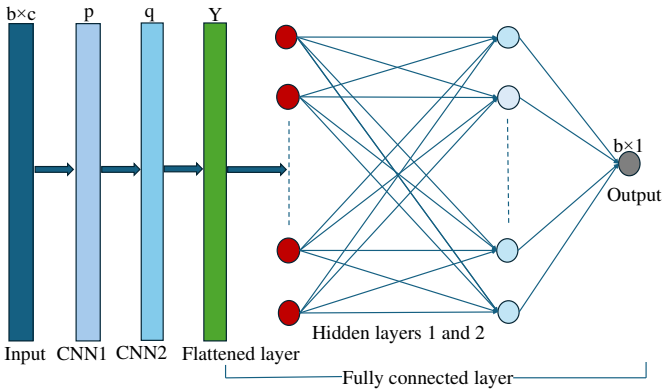

Fig. 3: Architecture of 1D CNN.

a hidden layer. The backpropagation updates the weights and biases according to the difference of error between the result obtained from CNN and the actual value given by six until the loss function reaches a minimum value and converges. The mean square error is evaluated as:

$$\text{MSE} = \frac{1}{N}\sum_{i=1}^{N}(x_i - \tilde{x}_i)^2 \tag{5}$$

$$w_{t+1} = w_t - \alpha\frac{\partial \text{MSE}}{\partial w_t} \tag{6}$$

The efficacy of the CNN is expressed in terms of root mean squared error. The frequency data obtained through the simulation and their implementation through CNN provide the inertia and damping constant estimation.

IV. Simulation and Results

A. Simulation Setup

The single-area power system of Fig. 1 is designed and simulated using MATLAB/Simulink 2023a. The data samples for $\Delta\omega$ and $\Delta\dot{\omega}$ are collected through simulation using the transfer function-based equivalent generator model. The data samples are collected by varying the inertia value from 2 seconds to 10 seconds with an interval of 0.5 while the excitation signal changes from 0.001 p.u. to 0.1 p.u., having a step size of 0.001 p.u. Similarly, the value of D varies from 0.5 to 2 with an increment of 0.15. A total of 1700 data samples are extracted for the estimation of inertia. The value of D is assumed to be 1.5 during the estimation of the inertia. Similarly, 1100 samples are utilized to estimate the coefficient of damping. The inertia is assumed to be 2.5 s during damping estimation. To make data more realistic, White Gaussian noise is implemented while simulating data samples in Simulink. A signal-to-noise ratio (SNR) of 65 dB, zero mean, and covariance of 1e-6 is used as explained in [24]. The CNN for inertia and damping constant is implemented in Python using Pytorch. The parameters utilized for the experiments are noted in Table I. The time interval equivalent to 1 second as described in [25] is chosen to make data measurement more realistic because it takes the system some duration to attain a steady state following the perturbation signal.

TABLE I: Simulation Parameters.

Parameters	**Ranges/Values**
Inertia constant (M)	2 s – 10 s Interval = 0.5 s
Damping coefficient (D)	0.5 – 2 Interval = 0.15 p.u.
Load (ΔP_L)	0.001 p.u. – 0.1 p.u. Interval = 0.001 p.u.
Speed regulation droop (R)	5%
Secondary controller gain (K)	2
Turbine-governor time constant (T_g)	0.25 s

B. CNN Structure and Hyperparameters Optimization

The sampling frequency equivalent to 200 Hz provides 200 samples within the inertial time interval of 1 second. The data obtained from the frequency measurements are standardized using the MinMax scalar to limit their values to 0 and 1. The batch size of 40 is maintained while training the entire dataset in each iteration. The CNN in this paper consists of one input layer, two convolution layers in the middle with kernels, three fully linked layers, and a final output layer. The number of channels and kernel size in each convolution layer are evaluated using Bayesian optimization. The range of values for the channels and kernel size are (10, 40) and (1,6), respectively. From the hyperparameter optimization, the optimized values for the number of channels are found to be 10 and 25, respectively, and the kernel size of 3 for each layer gave the optimized results. The kernel size is important since it determines the convolution filter size that moves across the input for retrieving the spatial aspects of the input sample. Thus, the first convolution layer has one input channel and ten output channels connected to another convolution layer, with 25 output channels ultimately connected to the first fully connected layer. The input to the first fully linked layer Y is calculated to be 9950 and input to the subsequent second and third levels are 800 and 50, respectively. The ReLU activation function is used for the convolution layers to add non-linearity to the model so that it helps in capturing the intricate features in the data. Similarly, the tangent hyperbolic function is used in the forward network. The weight update algorithm uses a momentum-accelerated gradient descent method with the weight decay factor. The optimized values for momentum, weight decay, and learning rate are 0.5, 1e-4, and 1e-5, respectively. In both of the estimations, the total dataset is divided in the ratio of 0.8/0.2 for training and testing data, respectively.

The inertia and damping constant training loss for the CNN are illustrated in Fig. 4. For the training of CNN for inertia estimation, the validation loss closely follows the training loss and losses decrease over the epochs, converging to the minimum value between 190 to 200 epochs as shown in Fig. 4a. Similarly, Fig. 4b demonstrates the MSE loss of training and validation datasets for the damping constant estimation. The early-stopping technique is utilized to stop the training process at epoch 200 to yield the optimal CNN model for the damping constant estimation process.

C. Analyzing Test Performance of CNN for Inertia and Damping Estimation

Fig. 5a shows the predicted values of the inertia constant on the testing set. The estimated values of the inertia have a root mean squared error (RMSE) of 0.2269. The scatter plot represents the distribution of estimated values at particular inertia points. It can be seen that most of the estimated values of the inertia are within the range of the actual values, demonstrating good estimation. However, the performance deteriorates towards the higher values of actual inertia, lowering the overall accuracy of the model. The median and quartile

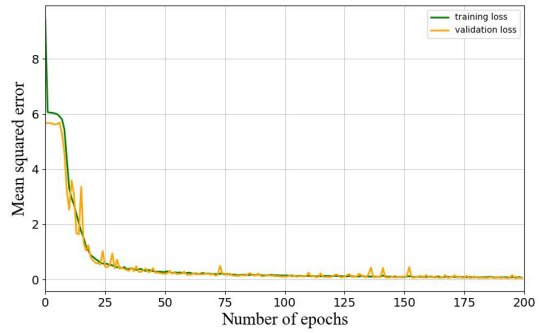

(a)

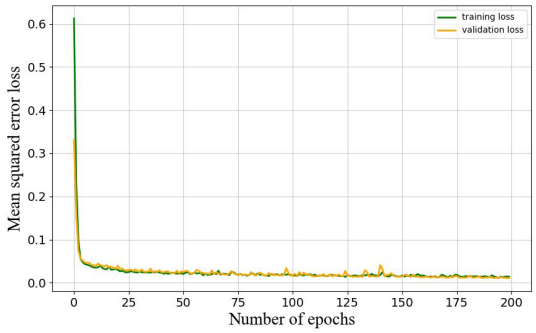

(b)

Fig. 4: Training loss function for a) inertia and b) damping constant estimation.

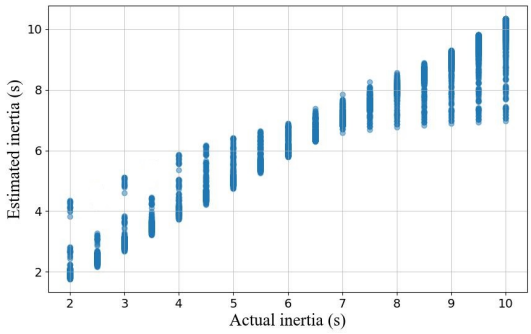

(a)

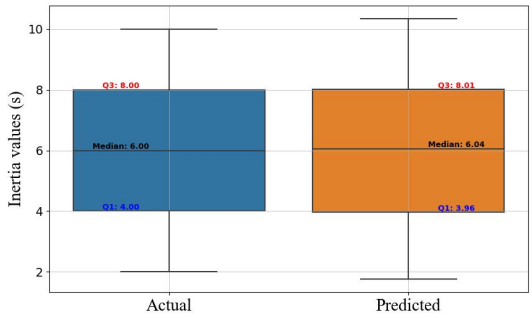

(b)

Fig. 5: a) Scatter graph b) Box plot of predicted and actual inertia constants.

values in Fig. 5b show a good agreement between the actual and predicted inertia values.

The scatter graph and box plot for estimated and true values of the damping constant are shown in Fig. 6. The model predicted the damping values with RMSE equivalent to 0.2563. As shown in Fig. 6a, most of the predicted values of the damping constant follow the actual values. The presence of outliers and more dispersion of data points affects the CNN performance. It can be seen that the CNN has a lower performance while estimating damping constants as there is a larger difference in predicted and estimated median and quartile values in Fig. 6b compared to the inertia estimation.

D. Comparision with other Machine Learning Models

Table II shows the performance of different off-the-shelf regression models in comparison to the proposed CNN model. It should be noted that while calculating the model accuracy, the predicted values of the inertia and damping with a tolerance of 10% are recognized as true values for all models. The performance of the CNN model is compared with the multi-layer perceptron, support vector machine regressor, and gradient-boosting machine regressor. The proposed CNN model outperforms the other model for all performance metrics. In MLP, each neuron is connected to every other neuron in the preceding layer, increasing the redundant parameters and complexity. As a result, MLP has limited ability to generalize and problems with convergence. The simpler architecture and limited feature parameters in SVR and GBM may be inad-

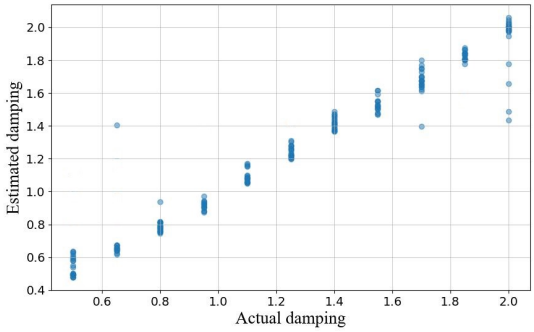

(a)

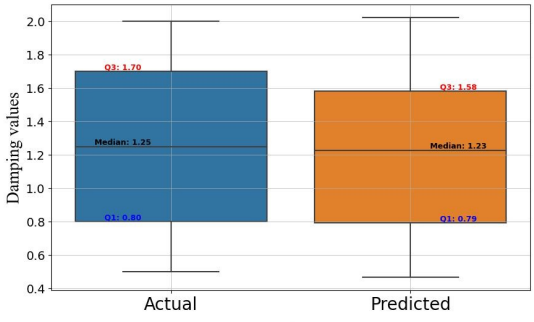

(b)

Fig. 6: a) Scatter graph b) Box plot of predicted and actual damping constants.

equate to reflect the complex relationship between frequency deviation and inertia. In addition to having significantly higher performance metrics, CNN uses the same set of weights (filter) across different input regions that reduce the parameters. This makes them efficient and scalable, allowing them to be trained on larger datasets with smaller computational complexity.

TABLE II: Test data performance metrics of different machine-learning models for inertia and damping estimation.

Parameter	Method	Accuracy	RMSE	MAE	R^2
Inertia	CNN	96.34%	0.2269	0.0891	0.977
	MLP	87.87%	0.2761	0.1924	0.898
	SVR	76.82%	0.45	0.3767	0.753
	GBM	75.29%	0.52	0.4517	0.748
Damping	CNN	94.32%	0.2563	0.0997	0.952
	MLP	85.17%	0.317	0.2178	0.859
	SVR	74.38 %	0.477	0.349	0.749
	GBM	72.29%	0.55	0.493	0.724

Thus, the proposed CNN model performed well in estimating the damping and inertia of the electrical grid. The testing accuracy and other matrices evaluated above clearly demonstrate the superiority of the model.

V. Conclusion

In this paper, the inertia, along with the damping, are estimated using the convolution neural network. The excitation signal is used to disturb the system's frequency dynamics, and frequency measurements obtained from probing are used as the input samples for the CNN training. The proposed model that is implemented in this paper is truly dependent upon the frequency data that has been obtained through disturbance in the system, making it a data-driven system. The model-free convolution neural network-based estimator displays high accuracy while estimating inertia and damping values even in the presence of noise, demonstrating the real-world applicability of the proposed method. The proposed model-free approach can also be implemented in the converter-dominated system to predict unknown inertia and damping constants. Future works involve extending the model to inherit the characteristics of renewable energy resources by incorporating their dynamics.

Acknowledgment

This material is based upon work supported by the National Science Foundation under an NSF CAREER Award Number 2339456.

References

[1] F. Milano, F. Dörfler, G. Hug, D. J. Hill, and G. Verbič, "Foundations and challenges of low-inertia systems," in *2018 Power Syst. Comput. Conf. (PSCC)*, pp. 1–25, IEEE, 2018.

[2] A. Robb, "Grid inertia: why it matters in a renewable world," *Renewable Energy World*, 2019.

[3] H. R. Chamorro, C. A. Ordonez, J. C. Peng, and M. Ghandhari, "Non-synchronous generation impact on power systems coherency," *IET Gener. Transmiss. Distribution*, vol. 10, no. 10, pp. 2443–2453, 2016.

[4] K. Yan, G. Li, R. Zhang, Y. Xu, T. Jiang, and X. Li, "Frequency control and optimal operation of low-inertia power systems with hvdc and renewable energy: A review," *IEEE Trans. Power Syst.*, vol. 39, no. 2, pp. 4279–4295, 2023.

[5] D. Zografos and M. Ghandhari, "Power system inertia estimation by approaching load power change after a disturbance," in *2017 IEEE Power & Energy Soc. General Meeting*, pp. 1–5, IEEE, 2017.

[6] P. Makolo, R. Zamora, and T.-T. Lie, "Online inertia estimation for power systems with high penetration of res using recursive parameters estimation," *IET Renewable Power Gener.*, vol. 15, no. 12, pp. 2571–2585, 2021.

[7] A. Ulbig, T. S. Borsche, and G. Andersson, "Impact of low rotational inertia on power system stability and operation," *IFAC Proceedings Volumes*, vol. 47, no. 3, pp. 7290–7297, 2014.

[8] E. Ørum, M. Kuivaniemi, M. Laasonen, A. I. Bruseth, E. A. Jansson, A. Danell, K. Elkington, and N. Modig, "Future system inertia," *ENTSOE, Brussels, Tech. Rep*, pp. 1–58, 2015.

[9] T. Inoue, H. Taniguchi, Y. Ikeguchi, and K. Yoshida, "Estimation of power system inertia constant and capacity of spinning-reserve support generators using measured frequency transients," *IEEE Trans. Power Syst.*, vol. 12, no. 1, pp. 136–143, 1997.

[10] M. Shamirzaee, H. Ayoubzadeh, D. Farokhzad, F. Aminifar, and H. Haeri, "An improved method for estimation of inertia constant of power system based on polynomial approximation," in *2014 Smart Grid Conf. (SGC)*, pp. 1–7, IEEE, 2014.

[11] X. Cao, B. Stephen, I. Abdulhadi, C. Booth, and G. Burt, "Switching markov gaussian models for dynamic power system inertia estimation," *IEEE Trans. Power Syst.*, vol. 31, no. 5, pp. 3394–3403, 2015.

[12] N. Petra, C. G. Petra, Z. Zhang, E. Constantinescu, and M. Anitescu, "A bayesian approach for parameter estimation with uncertainty for dynamic power systems," *IEEE Trans. Power Syst.*, vol. 32, no. 4, pp. 2735–2743, 2016.

[13] D. del Giudice and S. Grillo, "Analysis of the sensitivity of extended kalman filter-based inertia estimation method to the assumed time of disturbance," *Energies*, vol. 12, no. 3, p. 483, 2019.

[14] D. Yang, B. Wang, G. Cai, Z. Chen, J. Ma, Z. Sun, and L. Wang, "Data-driven estimation of inertia for multiarea interconnected power systems using dynamic mode decomposition," *IEEE Trans. Ind. Inform.*, vol. 17, no. 4, pp. 2686–2695, 2020.

[15] J. Zhang and H. Xu, "Online identification of power system equivalent inertia constant," *IEEE Trans. Ind. Electron.*, vol. 64, no. 10, pp. 8098–8107, 2017.

[16] P. Wall and V. Terzija, "Simultaneous estimation of the time of disturbance and inertia in power systems," *IEEE Trans. Power Del.*, vol. 29, no. 4, pp. 2018–2031, 2014.

[17] G. Cai, B. Wang, D. Yang, Z. Sun, and L. Wang, "Inertia estimation based on observed electromechanical oscillation response for power systems," *IEEE Trans. Power Syst.*, vol. 34, no. 6, pp. 4291–4299, 2019.

[18] A. Poudyal, R. Fourney, R. Tonkoski, T. M. Hansen, U. Tamrakar, and R. D. Trevizan, "Convolutional neural network-based inertia estimation using local frequency measurements," in *2020 52nd North American Power Symp. (NAPS)*, pp. 1–6, 2021.

[19] H. Bevrani, *Robust power system frequency control*. Springer, 2014.

[20] J. Schiffer, P. Aristidou, and R. Ortega, "Online estimation of power system inertia using dynamic regressor extension and mixing," *IEEE Trans. Power Syst.*, vol. 34, no. 6, pp. 4993–5001, 2019.

[21] M. Farrokhabadi, C. A. Cañizares, J. W. Simpson-Porco, E. Nasr, L. Fan, P. A. Mendoza-Araya, R. Tonkoski, U. Tamrakar, N. Hatziargyriou, D. Lagos, *et al.*, "Microgrid stability definitions, analysis, and examples," *IEEE Trans. Power Syst.*, vol. 35, no. 1, pp. 13–29, 2019.

[22] U. Tamrakar, T. M. Hansen, R. Tonkoski, and D. A. Copp, "Model predictive frequency control of low inertia microgrids," in *2019 IEEE 28th Int. Symp. Ind. Electron. (ISIE)*, pp. 2111–2116, IEEE, 2019.

[23] C. I. Garcia, F. Grasso, A. Luchetta, M. C. Piccirilli, L. Paolucci, and G. Talluri, "A comparison of power quality disturbance detection and classification methods using cnn, lstm and cnn-lstm," *Applied sciences*, vol. 10, no. 19, p. 6755, 2020.

[24] M. Brown, M. Biswal, S. Brahma, S. J. Ranade, and H. Cao, "Characterizing and quantifying noise in pmu data," in *2016 IEEE Power and Energy Soc. General Meeting (PESGM)*, pp. 1–5, 2016.

[25] A. Poudyal, U. Tamrakar, R. D. Trevizan, R. Fourney, R. Tonkoski, and T. M. Hansen, "Multiarea inertia estimation using convolutional neural networks and federated learning," *IEEE Sys. J.*, vol. 16, no. 4, pp. 6401–6412, 2022.